ChemInform Abstract: Withaferin A-Related Steroids from Withania aristata Exhibit Potent Antiproliferative Activity by Inducing Apoptosis in Human Tumor Cells.

ARTICLE *in* EUROPEAN JOURNAL OF MEDICINAL CHEMISTRY · JUNE 2012

Impact Factor: 3.45 · DOI: 10.1016/j.ejmech.2012.05.032 · Source: PubMed

European Journal of Medicinal Chemistry 54 (2012) 499–511

Contents lists available at SciVerse ScienceDirect

European Journal of Medicinal Chemistry

journal homepage: http://www.elsevier.com/locate/ejmech

Original article

Withaferin A-related steroids from *Withania aristata* exhibit potent antiproliferative activity by inducing apoptosis in human tumor cells

Gabriel G. LLanos [a], Liliana M. Araujo [b], Ignacio A. Jiménez [a], Laila M. Moujir [b], Isabel L. Bazzocchi [a,*]

[a] *Instituto Universitario de Bio-Orgánica "Antonio González" and Departamento de Química Orgánica, Universidad de La Laguna, Avenida Astrofísico Francisco Sánchez 2, 38206 La Laguna, Tenerife, Spain*
[b] *Departamento de Microbiología y Biología Celular, Universidad de La Laguna, Avenida Astrofísico Francisco Sánchez s/n, 38206 La Laguna, Tenerife, Spain*

GRAPHICAL ABSTRACT

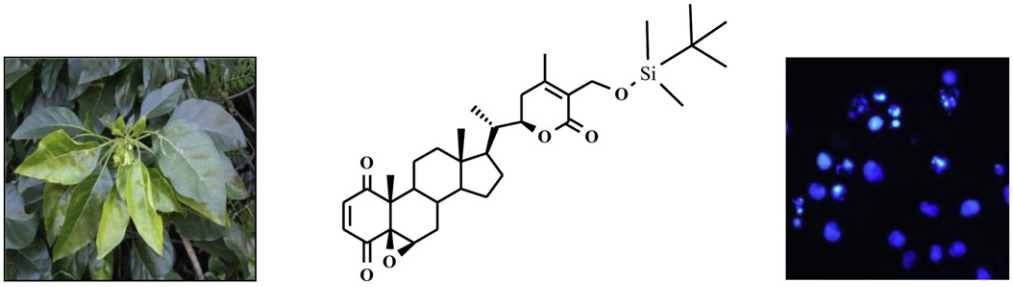

HIGHLIGHTS

- A series of new withanolides were isolated from *Withania aristata*.
- First examples of silyl ether–withaferin A derivatives.
- Five compounds of this series exhibited higher antiproliferative effects than withaferin A.
- Hoechst, Annexin V/PI and caspase-3 studies revealed that compounds induce apoptosis in HeLa cells.
- This study sheds more light on the potential of withanolides as anticancer agents.

ARTICLE INFO

Article history:
Received 20 January 2012
Received in revised form
18 May 2012
Accepted 23 May 2012
Available online 1 June 2012

Keywords:
Withania aristata
Withanolides
Antiproliferative
Human cancer cell lines
Apoptosis
Caspase-3
Structure–activity relationship

ABSTRACT

Six new withanolides (**1**–**6**) along with eleven known ones (**7**–**17**) were isolated from the leaves of *Withania aristata*. Their structures were elucidated on the basis of spectroscopic analysis, including 1D and 2D NMR techniques. Semisynthesis of the minority metabolites **7** and **15** from compounds **6** and **9**, respectively, as starting material, was performed. The isolated compounds as well as three derivatives (**7a**, **9a** and **9b**) of withaferin A were evaluated for cytotoxicity against HeLa (carcinoma of the cervix), A-549 (lung carcinoma) and MCF-7 (breast adenocarcinoma) human cancer cell lines, and against normal Vero cells (African green monkey kidney). Five compounds from this series (**8**, **9a**, **9b**, **11** and **13**) exhibited potent antiproliferative effects on the tumor cells, even higher than the well known anticancer agent, withaferin A (**9**). Phosphatidylserine externalization, chromatin condensation, and caspase-3 activation clearly indicated apoptosis as a mechanism of action. The structure–activity relationship revealed valuable information on the pharmacophore for withanolide-type compounds.

* Corresponding author. Tel.: +34 922 318594; fax: +34 922 318571.
E-mail address: ilopez@ull.es (I.L. Bazzocchi).

0223-5234/$ – see front matter
doi:10.1016/j.ejmech.2012.05.032

1. Introduction

Cancer still belongs to the second-leading cause of death worldwide. Because for many types of cancer no curative therapy is available, there is an ongoing need for novel leads for chemotherapy. Natural products represent a rich source of drug leads [1] and they have played a significant role in the discovery and development of new anticancer agents [2].

Withanolides are structurally diverse C_{28}-steroidal compounds built on an ergostane skeleton in which C-22 and C-26 are oxidized to form a δ-lactone ring on the nine-carbon side chain [3]. This class of steroids has attracted much interest due to their complex structural features, but also their broad range of biological activities [4].

Apoptosis is a fundamental and complex biological process in which cells play an active role in their own death. Dysregulation of apoptosis is the hallmark of all cancer cells and agents that activate programmed cell death could be valuable anticancer therapeutics [5].

Withaferin A, a prototype of the withanolides class of natural products, exerts its anticancer effect, through induction of apoptosis in a variety of human cancer cells, including prostate [6], colon [7], breast [8], leukemia [9], pancreatic [10], renal [11], head and neck [12], among others. It was shown that withaferin A actives p38 MAP kinase, inhibits the Notch signalling pathway and nuclear factor-κB activation [7,13], induces Akt inactivation, death receptor 5 (DR5) up-regulation and down-regulation of c-FLIP [11,14] as well as induces apoptosis through its ability to generate reactive oxygen species [15,16]. However, despite these advances, the precise mechanism by which withaferin A mediated cell death is not fully understood.

In the course of our search for bioactive metabolites isolated from species which grow in the Canary Islands, we focused our attention in *Withania aristata* (Ait.) Pauq. (Solanaceae), an endemic plant from Canary Islands, popularly known as "orobal". This species has long been used in traditional medicine as an antitumoral, antirheumatic and antispasmodic, as well as for insomnia, constipation and urinary pathologies [17] Previous phytochemical studies on *W. aristata* reported the isolation of six withanolides [18–22], and the cytotoxic [21] and diuretic activities [22] of withaferin A. Recently, we reported the isolation of seven new withanolides and their cytotoxicity against several human tumor cell lines [23].

In the present work, and as a continuation of our research directed at the discovery a novel drugs for treatment of cancer, we report herein on the isolation, structure elucidation and antiproliferative activity of six new (**1**–**6**) and eleven known (**7**–**17**) withanolides. In addition, the semisynthesis of the natural compounds **7** and **15** was carried out. The isolated compounds (**1**–**17**) and derivatives **7a**, **9a** and **9b** were evaluated against a representative panel of cancer cell lines, HeLa (carcinoma of the cervix), A-549 (lung carcinoma), and MCF-7 (breast adenocarcinoma), together with normal cells, Vero (African green monkey kidney) searching for selectivity. The present study was also undertaken to broaden the structural elements that are key for the efficient anticancer activity of this withanolide series. In order to investigate a possible mechanism for their antiproliferative effects, a series of experiments evaluating the induction of apoptosis in HeLa cells of the most active compounds **8**, **11**, **13**, **9a**, **9b** and withaferin A (**9**), was performed.

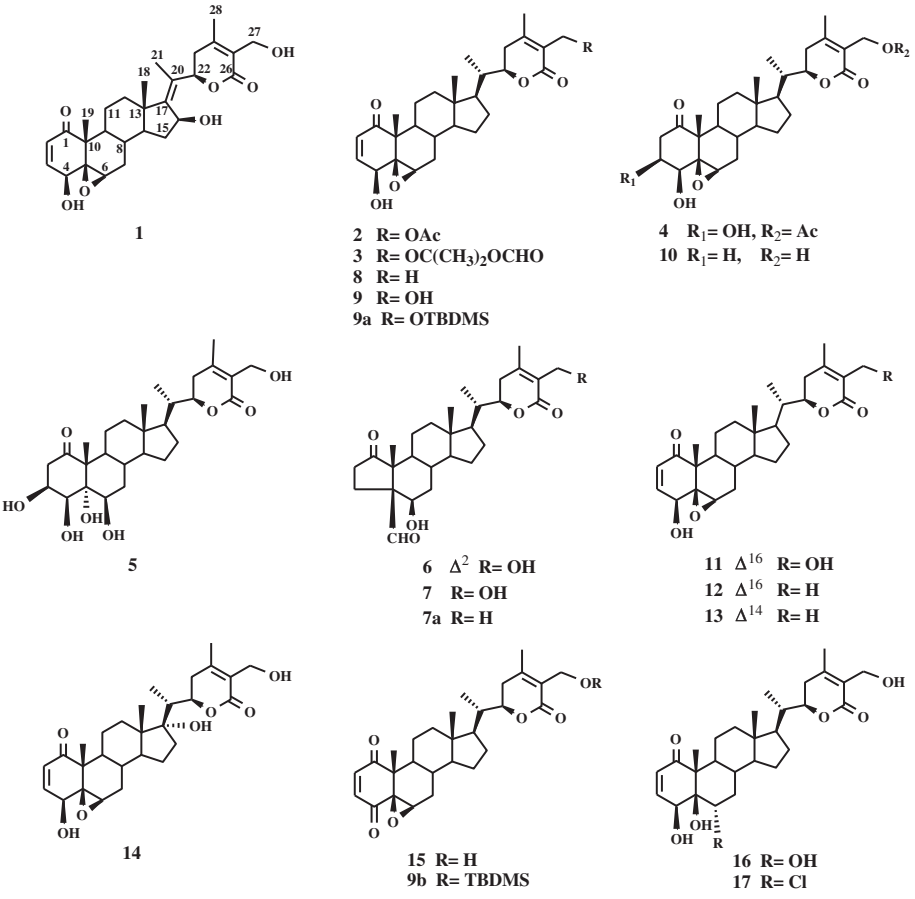

Fig. 1. Structure of natural withanolides (**1**–**17**) and derivatives (**7a**, **9a** and **9b**).

Table 1
^{1}H (400 MHz), and ^{13}C (100 MHz) NMR (δ, $CDCl_3$, J values in Hz in parentheses) data of compounds **1**–**4**.

No.	1		2		3		4	
	δ_H	δ_C[a]	δ_H	δ_C[a]	δ_H	δ_C[a]	δ_H	δ_C[a]
1		201.9 s		202.1 s		202.4 s		209.8 s
2	6.21 d (10.0)	132.0 d	6.21 d (10.0)	132.1 d	6.22 d (9.7)	132.3 d	2.53 dd (5.0, 15.4) 3.21 dd (6.4, 15.4)	42.5 t
3	6.95 dd (5.9, 10.0)	141.8 d	6.95 dd (5.9, 10.0)	141.7 d	6.95 dd (5.2, 9.7)	141.9 d	4.34 dd (4.2, 10.3)	68.5 d
4	3.77 d (5.9)	69.6 d	3.76 d (5.9)	69.6 d	3.79 d (5.2)	69.9 d	3.46 d (3.7)	76.3 d
5		63.7 s		63.6 s		63.9 s		64.2 s
6	3.26 br s	62.2 d	3.24 br s	62.3 d	3.26 br s	62.7 d	3.31 br s	60.1 d
7α	1.40 m	30.8 t	1.29 m	30.9 t	1.28 m	31.2 t	1.36 m	30.9 t
7β	2.21 m		2.15 m		2.16 m		2.20 m	
8	1.64[b]	28.4 d	1.53 m	29.5 d	1.54 m	29.4 d	1.44 m	29.0 d
9	1.11 m	43.8 d	1.02 m	43.9 d	1.05 m	44.1 d	1.33 m	42.3 d
10		47.5 s		47.4 s		47.7 s		50.2 s
11	1.51, 1.93 m	22.0 t	1.48, 1.83 m	21.9 t	1.52, 1.87 m	22.2 t	1.34, 1.53 m	21.8 t
12	1.50[b], 2.29 m	36.6 t	1.13, 2.00 m	39.1 t	1.14, 1.98 m	39.4 t	1.19[b], 1.94 m	39.2 t
13		44.2 s		42.3 s		42.6 s		42.7 s
14	1.50[b]	52.4 d	0.95 m	55.8 d	0.96 m	56.1 d	1.01 m	56.0 d
15	1.64[b]	36.0 t	1.18, 1.65 m	24.0 t	1.20, 1.67 m	24.3 t	1.19[b], 1.69 m	24.2 t
16	4.73 br s	71.5 d	1.38, 1.70 m	27.0 t	1.40, 1.68 m	27.3 t	1.40, 1.70 m	27.3 t
17		150.9 s	1.10 m	51.7 d	1.10 m	52.0 d	1.13 m	52.0 d
18	0.89 s	16.1 q	0.70 s	11.4 q	0.73 s	11.6 q	0.70 s	11.6 q
19	1.42 s	17.1 q	1.41 s	17.2 q	1.44 s	17.5 q	1.35 s	16.1 q
20		129.5 s	2.00 m	38.5 d	2.04 m	38.8 d	2.03 m	38.8 d
21	1.81 s	12.0 q	1.00 d (6.6)	13.1 q	1.02 d (6.2)	13.4 q	1.03 d (6.4)	13.3 q
22	5.37 dd (3.5, 12.9)	77.6 d	4.41 dt (3.3,13.2)	78.0 d	4.48 br d (13.4)	78.8 d	4.44 dt (3.0,13.3)	78.2 d
23α	2.23 m	34.5 t	2.01 m	29.8 t	2.03 m	30.0 t	2.05 m	30.1 t
23β	2.72 m		2.53 m		2.57 m		2.55 m	
24		153.5 s		156.8 s		156.7 s		157.0 s
25		125.1 s		121.6 s		123.0 s		121.9 s
26		166.7 s		165.2 s		167.9 s		165.3 s
27	4.38, 4.43 d_{AB} (12.6)	57.2 t	4.88, 4.92 d_{AB} (11.9)	57.8 t	4.27, 4.32 d_{AB} (10.0)	54.5 t	4.89, 4.92 d_{AB} (12.0)	58.0 t
28	2.02 s	19.6 q	2.08 s	20.4 q	2.10 s	20.5 q	2.11 s	20.6 q
				170.7 s		104.9 s		170.9 s
			2.06 s	20.7 q	1.46 s	22.4 q	2.09 s	20.9 q
					1.48 s	22.7 q		
					10.62 s	161.5 d		

[a] Data are based on DEPT, HSQC and HMBC experiments.
[b] Overlapping signals.

2. Results and discussion

2.1. Chemistry

The dichloromethane extract of the leaves of *W. aristata* was subjected to a series of column chromatography on silica gel and Sephadex LH-20, as well as preparative TLC and HPTLC, affording six new withanolides (**1**–**6**), along with the known ones **7**–**17** (Fig. 1).

Compound **1** was isolated as a white amorphous solid and showed the molecular formula $C_{28}H_{36}O_7$ by HREIMS. The EIMS displayed peaks at *m/z* 484 $[M]^+$, *m/z* 466 $[M^+ - H_2O]$, *m/z* 448 $[M^+ - 2\times H_2O]$ and *m/z* 343 $[M^+ -$ side chain]. The UV spectrum exhibited a strong absorption at 215 nm, indicating the presence of α,β-unsaturated carbonyl systems, and absorption bands for hydroxyl (3415 cm^{-1}), α,β-unsaturated carbonyl (1685 cm^{-1}) and epoxide (1180 cm^{-1}) groups were observed in its IR spectrum.

The ^{1}H NMR spectrum (Table 1) displayed an AMX system with signals at δ_H 6.21 (J_{AM} = 10.0 Hz), 6.95 (J_{MA} = 10.0 Hz, J_{Mx} = 5.9 Hz) and 3.77 (J_{xM} = 5.9 Hz), three oxymethine protons at δ_H 3.26 (br s) 4.73 (br s) and 5.37 (dd, J = 3.5, 12.9 Hz), and an oxymethylene at δ_H 4.38, 4.43 (d_{AB}, J = 12.6 Hz) as the most downshift signals. In addition, two singlet methyl groups at δ_H 2.02 and 1.81 attached to olefinic carbons, and two methyl groups at δ_H 0.89 and 1.42 were observed. Its ^{13}C NMR spectrum and DEPT experiments (Table 1) revealed 28 carbon signals, including an α,β-unsaturated ketone [δ_C 201.9 (C-1), 132.0 (C-2), 141.8 (C-3)], an α,β-unsaturated lactone [δ_C 153.5 (C-24), 125.1 (C-25), 166.7 (C-26)], two olefinic quaternary carbons [δ_C 150.9 (C-17), 129.5 (C-20)], three oxygenated methines [δ_C 69.6 (C-4), 71.5 (C-16), 77.6 (C-22)], an epoxide [δ_C 63.7 (C-5), 62.2 (C-6)], and one oxygenated methylene at δ_C 57.2 (C-27). These data indicated that compound **1** is an oxo-witha-trienolide, which presents, along with the usual unsaturations at C-2 and C-24, an additional one at C-17(20) suggested by the high chemical shifts of H-22 (δ_H 5.37) and Me-21 (δ_H 1.81) [24], and a hydroxyl group at C-16. The 16-hydroxy-17(20)-ene functional group is extremely uncommon in the withasteroid skeleton, and there are only two such withanolides found in nature [25]. These structural features

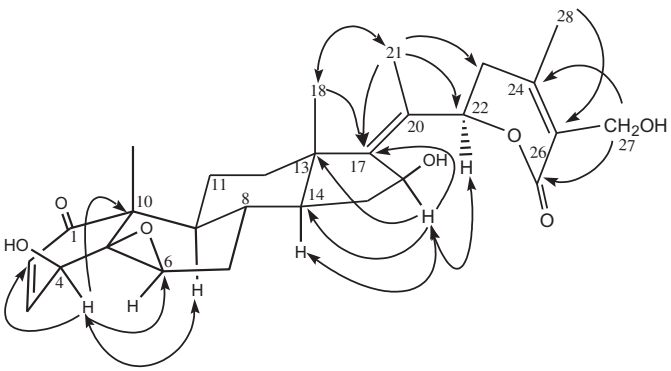

Fig. 2. ^{1}H-^{13}C long-range correlations (solid line) and ROE effects (dashed line) for compound **1**.

Table 2
^{1}H (400 MHz), and ^{13}C (100 MHz) NMR (δ, $CDCl_3$, *J* values in Hz in parentheses) data of compounds **5**–**7**.

No.	5		6		7	
	δ_H	δ_C[a]	δ_H	δ_C[a]	δ_H	δ_C[a]
1		209.8 s		208.9 s		216.2 s
2	2.53[b], 2.69 d (18.5)	41.4 t	6.55 d (5.8)	136.8 d	2.39, 2.57 m	32.5 t
3	4.38 m	72.9 d	6.97 d (5.8)	152.5 d	1.83[b], 2.03 m	22.5 t
4	4.46[b]	77.7 d	8.79 s	199.7 d	9.60 s	204.3 d
5		76.3[b] s		70.9 s		60.5 s
6	4.14 d (7.9)	76.3[b] d	4.58 br s	67.0 d	4.31 t (2.8)	67.4 d
7α	1.22[b]	31.8 t	1.00, 1.96 m	35.2 t	1.49, 1.87 m	33.9 t
7β	2.08 m					
8	1.58 m	30.9 d	1.89 m	30.1 d	1.83[b]	28.9 d
9	1.52 m	40.6 d	1.12 m	47.0 d	1.09 m	41.9 d
10		54.6 s		55.5 s		52.4 s
11	1.54 m	20.8 t	1.43 m	20.7 t	1.27[b], 1.67 m	22.4 t
12	1.11, 2.02 m	39.2 t	1.06 m	39.1 t	1.12, 2.02 m	39.1 t
13		42.7 s		42.9 s		43.0 s
14	1.01 m	57.8 d	0.94 m	55.8 d	1.08 m	55.7 d
15	1.22[b], 1.70 m	24.2 t	1.23, 1.64 m	23.9 t	1.27, 1.7[b]	23.9 t
16	1.41, 1.72 m	27.4 t	1.40, 1.66 m	27.1 t	1.43, 1.7[b]	27.1 t
17	1.15 m	51.6 d	1.09 m	51.7 d	1.16 m	51.7 d
18	0.72 s	11.6 q	0.77 s	11.7 q	0.77 s	11.7 q
19	1.26 s	14.7 q	1.22 s	12.1 q	1.19 s	13.1 q
20	2.05 m	38.8 d	2.00 m	38.5 d	2.04 m	38.5 d
21	1.02 d (6.5)	13.3 q	1.01 d (6.7)	13.1 q	1.03 d (6.6)	13.2 q
22	4.46[b]	78.8 d	4.41 dt (3.6, 13.3)	78.4 d	4.45 dt (3.5, 13.0)	78.5 d
23	2.00, 2.53[b] m	29.8 t	1.97 m, 2.51 t (12.4)	29.5 t	2.00, 2.54 m	29.5 t
24		153.3 s		153.3 s		152.5 s
25		125.6 s		125.5 s		125.5 s
26		167.2 s		166.7 s		166.8 s
27	4.36, 4.42 d_{AB} (12.4)	57.4 t	4.34, 4.40 d_{AB} (12.5)	57.2 t	4.37, 4.42 d_{AB} (12.3)	57.3 t
28	2.07 s	20.0 q	2.01 s	19.8 q	2.06 s	19.8 q

[a] Data are based on DEPT and HSQC experiments.
[b] Overlapping signals.

were confirmed by 2D NMR spectra. Thus, in its ^{1}H–^{1}H COSY spectrum, H-3 correlated with both H-2 and the oxygenated methine proton H-4, confirming the presence of a 4-hydroxy-2-en-1-one unit in the molecule. Also cross-peaking was found between H-6/H-7, H-15/H-16 and H-22/H-23.

The regiosubstitution of **1** was determined by an HMBC experiment (Fig. 2), showing as the most relevant three-bond correlations those of the proton resonance at δ_H 3.77 (H-4) with the signals at δ_C 132.0 (C-2), 62.2 (C-6) and 47.5 (C-10), correlation of the proton resonance at δ_H 4.73 (H-16) with the signals at δ_C 42.2 (C-13), 52.4 (C-14), 150.9 (C-17) and 129.5 (C-20), and those of the signal at δ_H 1.81 (Me-21) with the resonances at δ_C 150.9 (C-17) and 129.5 (C-20). The relative configuration of **1** was established on the basis of the coupling constants, molecular mechanic calculation using the PC Model [26] and confirmed by a ROESY experiment (Fig. 2). Thus, the β-hydroxyl group at C-16 was supported by molecular modelling of both α and β-epimers at C-16. The observed shape of the signal at δ_H 4.73 (H-16) as a broad singlet is closer to the values calculated for the 16β-hydroxy isomer [27], whereas an α orientation gives a larger *J* (9.0, 7.2 Hz) as previously reported for iochromolide [28], whose structure was confirmed by X-ray analysis. In the ROESY experiment a cross-peak of H-4 with H-9α and another of H-16 with H-14α and H-22α confirmed the β-stereochemistry of the hydroxyl groups at C-4 and C-16, while correlation of Me-21 with Me-18 and H-12 indicated a *Z* configuration of the double bond Δ^{17}. Thus, **1** was concluded to be 5β,6β-epoxy-4β,16β,27-trihydroxy-1-oxo-witha-2,17(20),24-trienolide.

Compound **2** showed a molecular formula of $C_{30}H_{40}O_7$ by HREIMS. Comparison of its NMR data (Table 1) with those of withaferin A (**9**) [29] indicated as the main difference the presence of an acetate group (δ_H 2.08, δ_C 20.7 and δ_C 170.7) instead of a primary alcohol. 2D NMR (COSY, ROESY, HSQC and HMBC) experiments allowed the complete and unambiguous assignment of the chemical shifts, regiosubstitution and relative configuration of compound **2**. Accordingly, the structure of **2** was established as 27-acetoxy-5β,6β-epoxy-4β-hydroxy-1-oxo-witha-2,24-dienolide (27-*O*-acetyl-withaferin A).

The HRESIMS of compound **3** indicated a molecular formula of $C_{32}H_{44}O_8$, and the ^{1}H and ^{13}C NMR data (Table 1) were closely related to those of **2**. Thus, the most notable differences were the

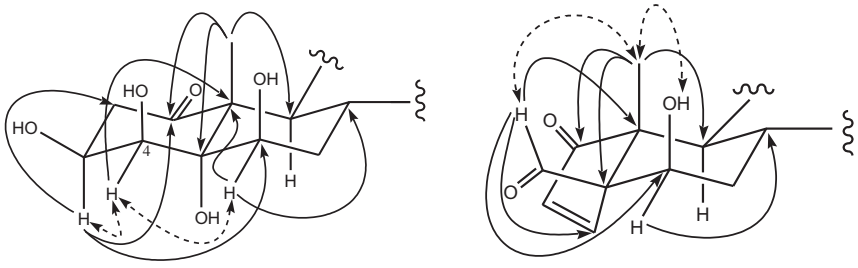

Fig. 3. ^{1}H-^{13}C long-range correlations (solid line) and ROE effects (dashed line) for compounds **5** (left) and **6** (right).

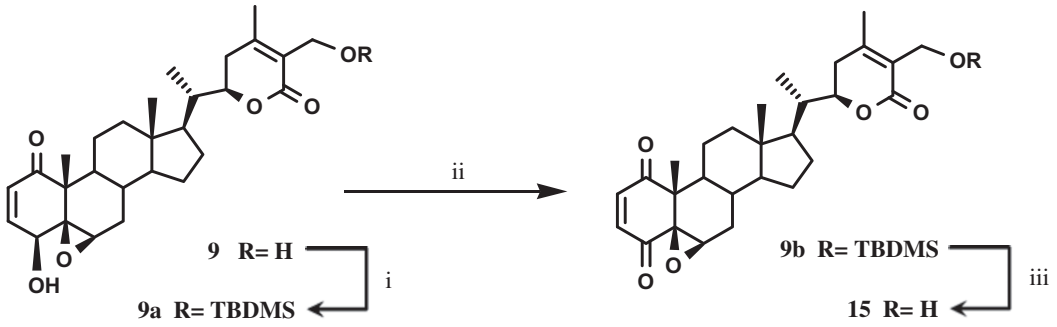

Scheme 1. Synthesis of derivatives **9a**, **9b** and **15**. Reagents and conditions: (i) TMDSCl, imidazole, DIMAP, CH_2Cl_2, r.t., 2.5 h; (ii) CrO_3, py, CH_2Cl_2, r.t., 6 h; (iii) Dowex (50WX8-200), acetone, r.t., 24 h.

presence of signals for two singlet methyl groups [δ_H 1.46 (3H, s), 1.48 (3H, s) and δ_C 22.4 (q), 22.7 (q)], a hemiketal carbon at δ_C 104.9 (s) and a formate group [δ_H 10.62 (1H, s) and δ_C 161.5 (d)] instead of the signals corresponding to the acetate group in **2**. Moreover, the 27-*O*-isopropyl formate group in **3** was located at C-27 as a result of the observed HMBC correlations of the primary alcohol resonance at δ_H 4.27, 4.32 (2H, d_{AB}, $J = 10$ Hz, H-27) and the aldehyde proton at δ_H 10.62 (1H, s) with the hemiketal carbon at δ_C 104.9. Therefore, the structure of compound **3** was deduced as 5β,6β-epoxy-4β-hydroxy-27-(1-formyloxy-1-methylethoxy)-1-oxo-witha-2,24-dienolide. To our knowledge, this is the first withanolide-type compound with an *O*-isopropyl formate moiety.

Compound **4** was assigned the molecular formula $C_{30}H_{42}O_8$ by HRESIMS, 18 mass units higher than that obtained for **2**. The ^1H and ^{13}C NMR data of **4** (Table 1) exhibited characteristic signals for a 5β,6β-epoxy-3β,4β-dihydroxy-1-one withanolide skeleton [30]. Its ^1H NMR data were similar to those of **2**, with the exceptions that signals were found for aliphatic methylene protons at δ_H 2.53 (dd, $J = 5.0$, 15.4 Hz), 3.21 (dd, $J = 6.4$, 15.4 Hz) assigned to H_2-2 and an oxymethine proton at δ_H 4.34 (dd, $J = 4.2$, 10.3 Hz, H-3) rather than the two olefinic protons of the α,β-unsaturated ketone of ring A in **2**. ^{13}C NMR resonances at δ_C 209.8 (C-1), 42.5 (C-2) and 68.3 (C-3) confirmed saturation of the C-2/C-3 bond and the presence of a hydroxyl group at C-3 in **4**. The location of the hydroxyl group at C-3 was also in agreement with the observed HMBC correlations of H-2 (δ_H 2.53)/C-1, C-3, C-4 and H-3 (δ_H 4.34)/C-1 and C-5 as well as those between H-4 (δ_H 3.46) and C-2, C-3, C-6 and C-10. The relative configuration of **4** was established on the basis of the coupling constants, molecular mechanic calculation using the PC model [26], comparison with the reported data in the literature [30] and confirmed by a ROESY experiment. Thus, the β-hydroxyl at C-3 was deduced by the coupling constants of H-3 [δ 4.34 (dd, $J = 4.2$, 10.3 Hz)] similar to those reported for 27-*O*-β-D-glucopyranosyl viscosalactone B [31]. Moreover, a cross-peak of H-6α with H-4α and one of H-4α with H-3 further confirmed the β-stereochemistry of the hydroxyl group at C-3. This spectral evidence determined the structure of **4** as 27-acetoxy-5β,6β-epoxy-3,4-dihydroxy-1-oxo-witha-24-enolide (27-*O*-acetyl-viscosalactone B).

The molecular formula of compound **5** was deduced to be $C_{28}H_{42}O_8$ by HRESIMS. A study of its IR, UV, ^1H and ^{13}C NMR (Table 2) and 2D spectra showed it to be a withanolide-type compound with a carbonyl group at δ_C 209.8 (C-1), a primary [δ_H 4.36, 4.42 (d_{AB}, $J = 12.4$ Hz, H-27) and δ_C 57.4 (C-27)], three secondary [δ_H 4.38 (m, H-3), 4.46 (m, H-4), 4.14 (d, $J = 7.9$ Hz, H-6), δ_C 72.9 (C-3), 77.7 (C-4), 76.3 (C-6)] and a tertiary [δ_C 76.3 (C-5)] hydroxyl groups, and an α,β-unsaturated δ-lactone moiety [δ_C 153.3 (C-24), 125.6 (C-25), 167.2 (C-26)]. The analysis of HMBC and ROESY experiments revealed that **5** have the same substitution pattern

Table 3
Cytotoxic activity (IC_{50}, μM) of withanolides[a] against tumor cell and Vero cell lines.

Compound	HeLa		A-549		MCF-7		Vero		SI[c]
	48 h	72 h	48 h	72 h	48 h	72 h	48 h	72 h	
1	40.0 ± 2.1	31.1 ± 2.6	>40	>40	27.7 ± 2.0	6.0 ± 0.1	>40	>40	<1
2	7.7 ± 0.3	4.7 ± 0.5	6.7 ± 0.1	4.4 ± 0.1	5.3 ± 0.1	2.0 ± 0.05	11.4 ± 0.7	8.5 ± 0.09	2.2
3	>40	37.3 ± 2.4	>40	>40	26.9 ± 1.5	18.3 ± 0.9	27.8 ± 1.5	18.5 ± 0.9	1.0
4	8.9 ± 0.3	8.3 ± 0.3	18.4 ± 0.7	21.3 ± 1.8	9.2 ± 0.2	7.1 ± 0.4	8.6 ± 0.1	4.9 ± 0.1	<1
8	4.6 ± 0.3	3.4 ± 0.06	9.0 ± 0.2	1.5 ± 0.05	6.6 ± 0.08	1.1 ± 0.02	1.5 ± 0.04	2.2 ± 0.03	<1
9	3.0 ± 0.1	2.3 ± 0.03	6.6 ± 0.08	1.5 ± 0.05	3.6 ± 0.02	0.6 ± 0.002	1.3 ± 0.005	1.7 ± 0.04	<1
10	28.9 ± 3.2	19.3 ± 0.7	33.5 ± 1.9	17.2 ± 0.8	14.4 ± 0.9	5.4 ± 0.1	15.5 ± 0.9	9.0 ± 0.3	1.1
11	3.5 ± 0.2	2.7 ± 0.06	4.2 ± 0.9	2.3 ± 0.06	1.2 ± 0.01	0.3 ± 0.003	3.4 ± 0.08	2.6 ± 0.2	2.8
12	21.5 ± 0.9	8.0 ± 0.1	40 ± 2.1	5.5 ± 0.2	12.6 ± 0.9	2.2 ± 0.008	4.7 ± 0.09	3.1 ± 0.06	<1
13	3.5 ± 0.1	2.9 ± 0.03	2.6 ± 0.04	2.1 ± 0.04	1.3 ± 0.07	0.3 ± 0.002	6.2 ± 0.1	1.2 ± 0.02	1.7
14	17.7 ± 0.9	19.8 ± 0.7	>40	31.7 ± 2.5	16.3 ± 1.1	10.3 ± 0.9	28.8 ± 1.7	21.8 ± 1.5	1.8
15	18.4 ± 1.0	15.2 ± 0.9	25.4 ± 1.8	12.8 ± 0.9	3.2 ± 0.3	2.1 ± 0.6	7.7 ± 0.3	1.5 ± 0.4	2.4
16	>40	31.4 ± 2.1	>40	36.4 ± 3.1	38.4 ± 2.8	36.2 ± 2.3	40 ± 2.1	26.9 ± 2.1	1.0
17	13.4 ± 0.7	12.1 ± 0.6	14.7 ± 0.7	8.6 ± 0.7	7.5 ± 0.1	1.3 ± 0.01	14.8 ± 1.0	7.8 ± 0.2	2.0
9a	0.9 ± 0.01	1.0 ± 0.04	1.5 ± 0.02	1.5 ± 0.03	0.7 ± 0.01	0.7 ± 0.006	0.7 ± 0.01	0.9 ± 0.01	1.0
9b	1.7 ± 0.01	2.1 ± 0.08	5.3 ± 0.3	2.9 ± 0.1	0.5 ± 0.01	0.2 ± 0.008	3.1 ± 0.1	4.0 ± 0.09	6.2
C1[b]	$1.1 \pm 0.1 \times 10^{-3}$	–	$7.2 \pm 0.3 \times 10^{-3}$	–	$2.4 \pm 0.1 \times 10^{-2}$	–	$7.1 \pm 0.5 \times 10^{-2}$	–	3.0
C2[b]	2.9 ± 0.06	–	47.0 ± 1.9	–	1.4 ± 0.06	–	67.6 ± 5.2	–	48.3

–: Not tested.
[a] Compounds **5**–**7** and **7a** showed $IC_{50} > 40$ μM against all the tested cell lines.
[b] C1 and C2: actinomycin and mercaptopurine, respectively, were used as positive controls.
[c] SI: Selectivity index defined as Vero (IC_{50}) on MCF-7.

and stereochemistry as viscosalactone B [30] with the only difference being a 5α,6β-diol system rather than the 5β,6β-epoxy group. Moreover, the localization of the two hydroxyl groups at C-5 and C-6 were determined as a result of the observed HMBC correlations between H-3/C-1, C-5; H-4/C-2, C-6, C-10; H-6/C-8, C-10 and Me-19/C-1, C-5, C-9 (Fig. 3). The stereochemistry of the hydroxyl group at C-5 was deduced as α, and therefore a *cis*-A/B ring junction, because no upfield shift effect was observed for the CH_3-19 (δ_C 14.7), whereas the presence of a 5β-OH does cause a 10 ppm upfield shift of CH_3-19 (around δ_C 9) due to the gauche-interaction [32]. Furthermore, the ROE correlations observed of H-4α with H-3 and H-6 defined the 6β-axial disposition for the hydroxyl group at C-6 (Fig. 3). Therefore, the structure of **5** was established as 3β,4β,5α,6β,27-pentahydroxy-1-oxo-witha-24-enolide. This compound has one feature of particular interest as it is the first withanolide-type compound reported with four hydroxyl groups on A/B rings.

Compound **6** showed spectral data resembling those of the known isolated compound **7** [33], and its molecular formula ($C_{28}H_{38}O_6$), determined by HRESIMS, revealed it to be 2 *m/z* lower than the one for **7**. The ^1H and ^{13}C NMR spectra suggested that **6** had a double bond at C2–C3 instead of a methylene group, as in **7**. Even so, it should be noted that a complete set of 2D NMR spectra (COSY, HSQC and HMBC) was acquired for **6** in order to gain the complete and unambiguous assignment of the ^1H and ^{13}C NMR resonances as listed in Table 2. The relative stereochemistry was confirmed by a ROESY experiment (Fig. 3). Thus, ROE correlation between the signal at δ_H 1.22 (Me-19) and the signals at δ_H 8.79 (CHO-4) and δ_H 3.27 (HO-6) established the β-orientation of the 4-formyl and 6-hydroxyl moieties. Therefore, the structure of compound **6** was determined to be 4β-formyl-6β,27-dihydroxy-1-oxo-witha-2,24-dienolide.

The conditions leading to the rearrangement that produced ring-A contraction and the formation of an aldehyde centre at C-4 have been reported previously in the literature [33]. Accordingly, compound **7** was obtained by treatment with sulphuric acid in acetone of 2,3-dihidrowithaferin A, however, as a natural compound, it is reported here for the first time. Although some of the ^1H and ^{13}C NMR data have already been published, we contribute with the complete and unambiguous assignments of the ^1H and ^{13}C NMR signals (Table 2) of the known withanolide 4β-formyl-6β,27-dihydroxy-1-oxo-witha-24-enolide (**7**) [33], based on 1D and 2D NMR techniques.

By comparing the NMR and MS data with those previously reported, eleven known compounds were identified as 4β-hydroxy-1-oxo-5β,6β-epoxywitha-2,24-dienolide [34] (**8**), withaferin A [27] (**9**), 2,3-dihydro-withaferin A [19] (**10**), witharistatin [21] (**11**), 27-deoxy-16-en-withaferin A [35] (**12**), 4β-hydroxy-1-oxo-5β,6β-epoxy-22*R*-witha-2,14,24-trienolide [19] (**13**), 5β,6β-epoxy-4β,17α,27-trihydroxy-1-oxowitha-2,24-dienolide [36] (**14**), 4-dehydro-withaferin A [29] (**15**), 2,3-dehydrosomnifericin [37] (**16**) and 6α-chloro-5β-hydroxywithaferin A [20] (**17**).

Owing to the fact that compounds **7** and **15** were isolated in insufficient amounts for the full biological evaluation, we decided to carry out their semisynthesis starting from withaferin A (**9**) and **6**, respectively (Scheme 1). Thus, catalytic reduction of compound **6** with palladium hydroxide-carbon gave compounds **7** and the known derivative **7a** [33]. Moreover, firstly, selective protection of the primary alcohol in compound **9** with TMDSCl, imidazole and DMAP in CH_2Cl_2 at room temperature during 2.5 h gave the corresponding silyl ether derivative (**9a**), which was then oxidized with CrO_3 in pyridine (Collins reagent) to afford the ketone **9b**. Further cleavage of the TBDMS group was achieved with carboxylic acid resin Dowex 50WX8-200 in acetone to yield compound **15**.

2.2. Biological evaluation

2.2.1. Antiproliferative activity

In our previous study on the biological activities of *W. aristata* extracts, the CH_2Cl_2 fraction showed a strong antiproliferative effect on two tumor cell lines, HeLa and A-549, with IC_{50} values of 11.7 and 19.9 μg/mL, respectively. This has encouraged us to investigate the isolates from this fraction for their cytotoxic activity.

In this study, the seventeen isolated compounds (**1**–**17**), including withaferin A (**9**) for comparative purposes, and three derivatives (**7a**, **9a** and **9b**) were assayed for their antiproliferative activity against three human cancer cell lines: HeLa (cervix), A-549 (lung) and MCF-7 (breast), and Vero (African green monkey kidney) non-tumoral cell line used for selectivity purposes. Except for the prototype withaferin A, few studies on the cytotoxic activity of the known isolated compounds **8** [38], **10** [21,39,40], **12** [38], **13** [21], **14** [38] and **15** [40] have been previously reported. Nevertheless, we include these compounds in our studies in order to broaden the structure–activity studies and, moreover, because the cell lines and procedures were different from the ones used herein.

As shown in Table 3, the silyl ether derivatives **9a** and **9b** showed pronounced antiproliferative activity against the tested tumor cell lines with IC_{50} values ranging from 0.5 to 2.9 μM, which are lower than those of the widely known anticancer withaferin A (IC_{50} 3.0–6.6 μM). Furthermore, compounds 27-*O*-acetyl-withaferin A (**2**), 4β-hydroxy-1-oxo-5β,6β-epoxywitha-2,24-dienolide (**8**), 16-en-withaferin A (**11**) and 4β-hydroxy-1-oxo-5β,6β-epoxy-22*R*-witha-2,14,24-trienolide (**13**) also displayed strong cytotoxicity, with IC_{50} values less than 9 μM. Among them, compounds **11** and **13** demonstrated stronger cytotoxicity against A-549 and MCF-7 cell lines than the reference, withaferin A. In addition, compounds **15** and **17** exhibited a fair level significant of activity against MCF-7 cells, with IC_{50} values of 3.2 and 7.5 μM, respectively. Overall, the compounds showed time dependent antitumoral activity against the investigated cell lines. Thus, compounds **8** and **13**, as did withaferin A, showed a significant increase in cytotoxicity (more than three-fold) against two or three human cancer cell lines after 72 h of exposure compared to 48 h.

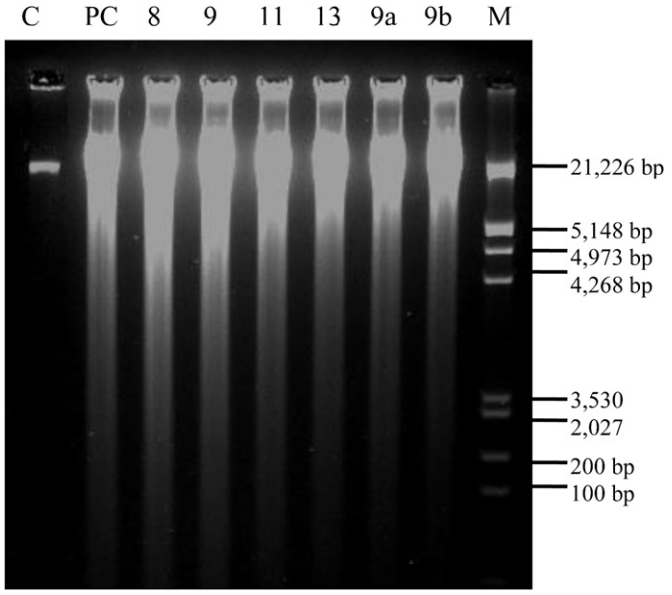

Fig. 4. Fragmentation of genomic DNA in HeLa cells. Cells were treated with compounds **8**, **9**, **9a**, **9b**, **11** and **13** at 16 μM for 48 h. agarose gel electrophoresis, visualized by ethidium bromide staining. Lane 1, untreated cells (C); PC, staurosporine at 2 μM (positive control); lanes 3–8, treatment with compounds **8**, **9**, **11**, **13**, **9a**, and **9b**, respectively; M, DNA marker of 125-21, 226 bp.

Moreover, MCF-7 cell line turned out to be the most sensitive to the withanolides.

In addition, when comparing MCF-7 cancer cells with the non-tumorigenic (Vero) cell line, some degree of selective cytotoxicity was observed (Table 3). Thus, the most active compound (**9b**) exhibited a selectivity index (SI) of 6.2 for this cell combination, higher than that withaferin A (SI 0.4). Moderate selectivity (SI $\geq$ 2) was also found for withanolides **2**, **11**, **15** and **17**, which may shed light on these compounds for future studies.

2.2.2. SAR analysis

The influence of the substitution pattern on the cytotoxic activity of the withanolides studied in this work was examined, revealing the following trends in the structure–activity relationship. a) The influence of substituents on the A and B rings was evident when we compared the activity displayed by **9** with those of **4**-**7**, **7a**, **8**–**10** and **16**–**17**, as simple modification of the double bond at C-2(3) (**9** *vs* **10**) or epoxy group at C-5(6) (**9** *vs* **16**) produced a considerable decrease in the activity. Moreover, the elimination of

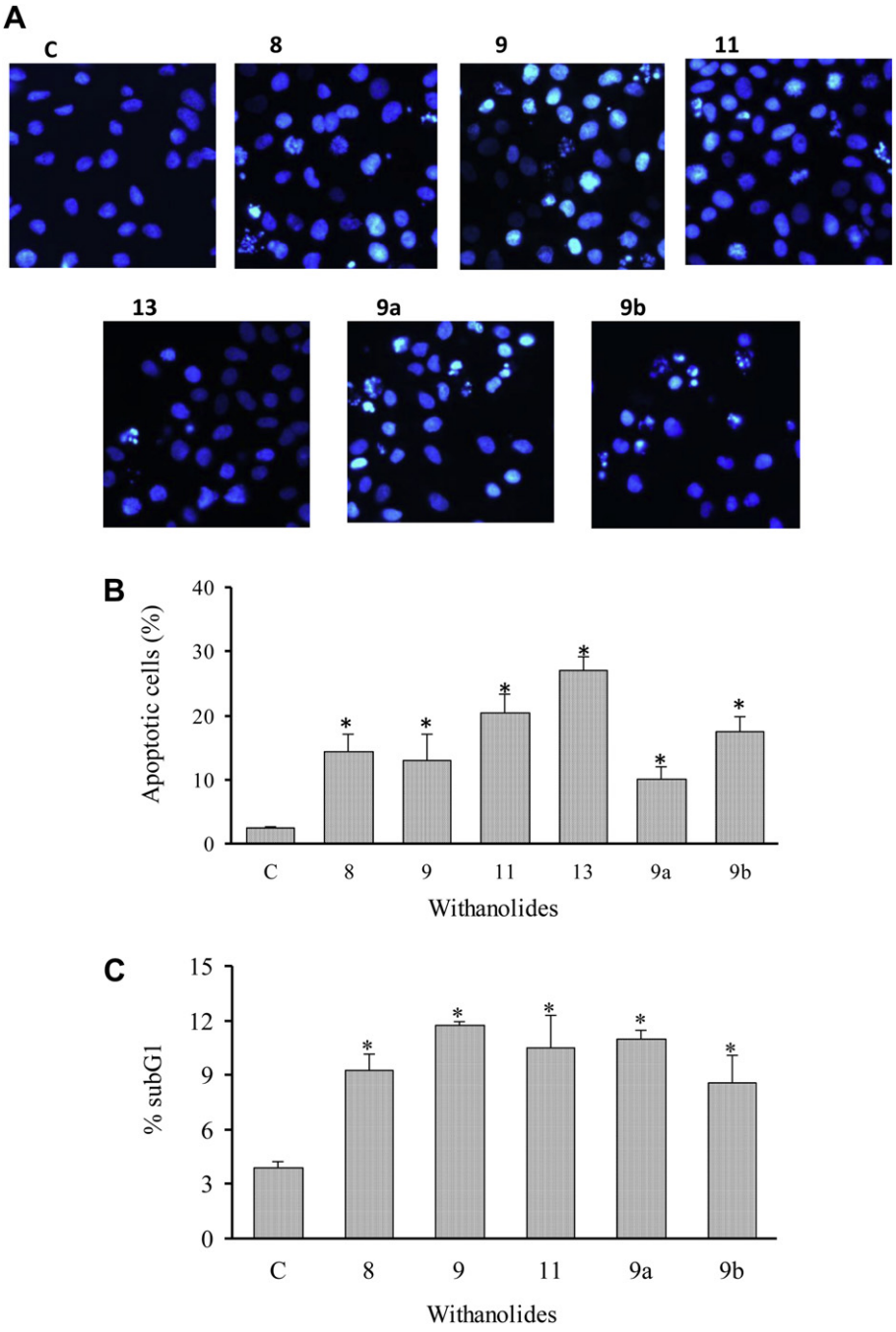

Fig. 5. Withanolide induced apoptotic nuclei in HeLa cells. (**A**) Representative fluorescence images of apoptotic nuclei. Cells were treated with the compounds **8**, **9**, **11**, **13** **9a** and **9b** at 8 μM or with the respective solvent control (C) for 12 h and then stained with Hoechst 33342; amplification 40×. (**B**) Percent of Hoechst-stained, apoptotic cells, calculated from a total of at least 500 per sample. Bars represent means ± SD of three independent experiments, performed in triplicates; $^{*}p < 0.05$. (**C**) Assessment of sub-G1 DNA content. Cells were incubated in the absence (control) versus presence of 24 μM of compounds **8**, **9**, **11**, **9a** and **9b** for 12 h, permeabilized, stained with propidium iodide, and analyzed by flow cytometry. Bars represent means ± SD of percent of cells undergoing apoptosis in each sample. Three independent experiments, each in triplicate, were performed. $^{*}p < 0.05$ with respect to controls.

those both essential groups, as in **5**, caused the abolition of cytotoxicity. These results are in agreement with previous studies [41,42], which define these functions as structural requirements in withanolide skeleton for biological function. However, in contrast with previous results [43], we found that the cytotoxic effect of the 6-chlorowithanolide **17** was higher than its corresponding hydroxyl derivative **16**. Furthermore, the most striking result was the replacement of a hydroxyl by a carbonyl group at C-4 which results in a considerable increase of selectivity (**9** *vs* **15** and **9a** *vs* **9b**).

a) Substituents on the five member ring play an important role and thus, comparison of the activity displayed by **8** and **9** with those of **1** and **11**–**14** showed as most relevant result the improvement of the Δ^{14}-withanolide **13.** On the other hand, a detrimental effect was observed with the presence of a hydroxyl group (**9** *vs* **1** and **14**).
b) Regarding the substituents on the lactone ring, we conclude that the substitution of a C-27 methyl (**8** and **12**) by a hydroxymethyl group (**9** and **11**) or substitution of a hydroxymethyl by a silyl ether (**9a** and **9b**) increases considerably the activity, whereas the presence at C-27 of an acetyl or ketal group (**2** and **3**) is detrimental. These trends, based upon substitution patterns, on one hand are consistent with previous SAR findings, and on other provide valuable information on the pharmacophore for withanolide-type compounds and will be helpful for the rational design of more potent and selective anticancer drugs.

2.2.3. Detection of apoptosis

The control of apoptosis is a crucial target for conventional drug development, particularly for cancer therapeutics. In this work, we employed various experimental approaches to characterize the apoptotic potential of the withanolides **8**, **9a**, **9b**, **11** and **13** in comparison with the structurally related well-known steroidal lactone withaferin A (**9**) in HeLa cervical carcinoma cells.

To start with, we tried to detect regular fragmentation of nuclear DNA, a phenomenon associated with most types of late stage apoptosis. HeLa cells were treated with withanolides at 16, 24, and 32 μM for 24 h and at a concentration of 16 μM for 48 h. Additionally, withaferin A was added to HeLa cultures at concentrations of 4, 8, 12, 16, 24, and 32 μM for 12 h. None of these treatments resulted in the typical DNA fragments of 180–200 bp and multiples, product of enzymatic cleavage. However, a predominant smear pattern in agarose gel electrophoresis was detectable with all test compounds (Fig. 4) at all concentrations and exposure times, also after treatment with withaferin A (data not shown), where induction of apoptosis has been described by various authors [5,15,16]. Similar results were obtained under actinomycin D and staurosporine treatment, substances known to induce apoptosis in many cell lines. The pattern was not evident in solvent control cultures.

In accordance with Meyer et *al.* [44], the apoptosis-specific 200-bp DNA ladder is overlaid by random DNA fragmentation, resulting from necrotic cell death, which may also appear in imiquimod or actinomycin D treated cell cultures. While rapidly removed by phagocytosis *in vivo*, apoptotic bodies are usually not eliminated in cell cultures and finally lyse, leading to a state of secondary necrosis. Thus, DNA fragmentation is common to different kinds of cell death; three types of DNA fragmentation can occur during apoptosis: internucleosomal DNA cleavage, fragmentation into large fragments of 50–300 kbp length, and single-strand cleavage events [45].

In view of these observations, we decided to check for chromatin condensation, a hallmark of apoptosis, where compact and small chromatin nuclei and often apoptotic bodies appear. To this end, HeLa cells were exposed to the withanolides at 8 μM for 12 h and the morphological features of apoptotic cells were determined by staining with Hoechst 33342, a specific stain for AT-rich regions of double-stranded DNA. Condensation of chromatin and apoptotic bodies in the vicinity of the cells were clearly observed by fluorescence microscopy (Fig. 5A), which suggests induction of apoptotic cell death by all withanolides. Apoptotic cells were quantified taking into account only those cells the chromatin of which had split into more than three fragments. The number of apoptotic cells was significantly higher upon treatment with the withanolides than in the control cells ($p < 0.05$) and even higher than upon withaferin A treatment, as approximately 27% more apoptotic cells were assessed in the withanolide **13** samples (Fig. 5B).

Additionally, the degree of induced apoptosis was estimated by flow cytometry evaluation of the characteristic sub-G1 peak, which reflects cells with a lower DNA content compared to cells in G0/G1 phase of the cell cycle [46,47]. Except for withanolide **13**, where we had run out of compound, cell exposure to all the withanolides at 24 μM for 12 h produced defined sub-G1 peaks (Fig. 5C).

However, chromatin condensation may also be found in necrotic cells [48]. Moreover, apoptosis and necrosis are two types of demise that can occur simultaneously in tissues or cell cultures exposed to a single stimulus. Often, the intensity of the initial insult decides for the prevalence of either apoptosis or necrosis. Hence, the evaluation of proteins, implicated in activation or execution of apoptosis, may help unravel the type of ongoing cell death. Caspases are crucial mediators of programmed cell death (apoptosis). Among them, caspase-3 is a commonly activated death effector protease, catalyzing the specific cleavage of various key cellular proteins. Its role in programmed cell death has been shown to be remarkably tissue- cell type-, or death stimulus- specific. Caspase-3 activation is essential for some of the characteristic changes in cell

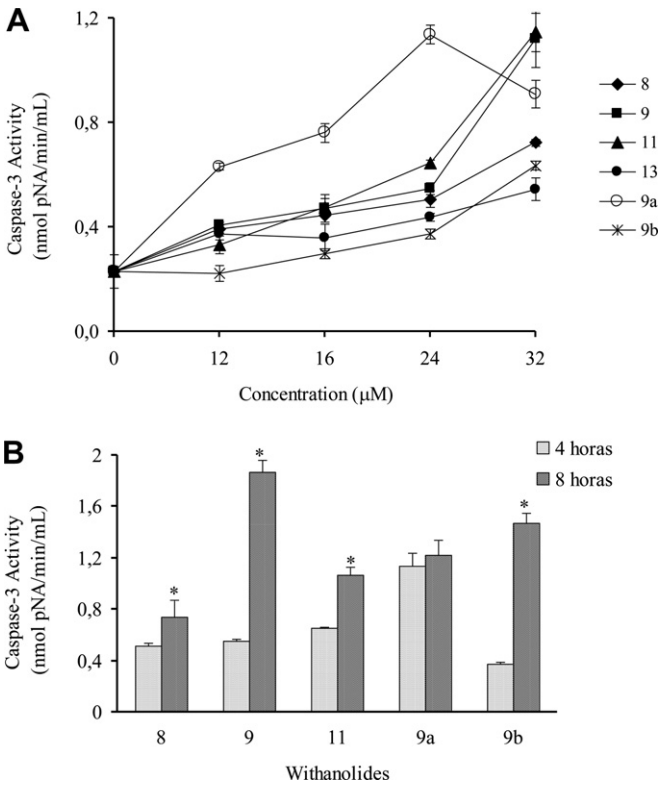

Fig. 6. Caspase-3 activity in HeLa cells. (**A**) Cells treated with compounds **8**, **9**, **11**, **13**, **9a** and **9b** at 12, 16, 24, and 32 μM for 4 h. (**B**) Cells treated with the same compounds (except compound **13**) at 24 μM for 4 and 8 h, respectively. Values represent means ± SD of three independent experiments, each performed in triplicate; difference between treatments and control with $p < 0.05$ (*) was considered statistically significant.

morphology and certain biochemical events associated with the execution and completion of apoptosis [49] and eventually lead to degradation of chromosomal DNA [50].

Withaferin A has been reported to activate the apoptotic cascade by extrinsic or intrinsic pathways in promyelocytic leukemia cells HL-60 [51], U937 [14] prostate cancer [52], and HNSCC cells [11] among others. Hence, we wished to definitely identify the type of ongoing cell death in HeLa cells, determining potential caspase-3 activation by withanolides **8**, **9**, **11**, **13, 9a** and **9b**. The induction of caspase-3 was assessed by colorimetric assay after treatment of HeLa cells with the withanolides at different concentrations (4, 8, 12, 16, 24, and 32 μM) for 4 h Fig. 6A shows that the withanolides induced caspase-3 activation in a dose-dependent manner in concentrations >12 μM, while enzyme activity at 4 and 8 μM did not differ from untreated cells. Particularly, withaferin A and **11** increased enzyme activity from 1 to 2 fold at 12 μM, respectively (compared to controls) to 5-fold at 32 μM. Notably, caspase activity declined upon treatment with withanolide **9a** at 32 μM for 4 h, which was probably due to the associated loss of cellular integrity and adhesion, as observed by light microscope (data not shown).

To determine whether caspase-3 activation could further increase with time, HeLa cells were treated with compounds **8**, **9**, **11**, **9a** and **9b** at a fixed concentration of 24 μM for 8 h. In fact, caspase-3 activity further augmented with 8 h, mainly after exposure to withaferin A and **9b** that produced activities similar to the one with staurosporine treatment at 2 μM for 4 h (1.92 nmol pNA/min/mL ± 0.13), used as positive control (Fig. 6B). Again, treatment with **9a** only induced a negligible increase in caspase-3 activity, associated with drastic cell damage.

The early stage of apoptosis is typically accompanied by a loss of membrane phospholipid asymmetry, going along with phosphatidylserine (PS) flipping onto the surface of the cell. PS externalization plays an important role in the recognition and removal of apoptotic cells by macrophages [53]. Therefore, we decided to use annexin V, a specific ligand of PS, to determine the early apoptotic fraction in HeLa cells and propidium iodide (PI), which can only pass the cell membrane in late stage apoptosis or necrosis. HeLa cells were exposed to withanolides at a concentration range of 2–16 μg/mL for 30 min, 1, 2, and 4 h of incubation before costaining with annexin V/PI. Fluorescence microscopy (Fig. 7) evidenced that, in contrast to untreated cells, all withanolides, as well as the positive control actinomycin D, induced dose- and time-dependent PS externalization and/or necrosis in HeLa cells. Early apoptotic cells (annexin V+) were evidenced after treatment with compounds **8**, **9**, and **11** at 2 and 4 μM over a period of 4 h, while exposure to **13** led to early and late apoptosis (annexin V+/PI+) in these conditions. A higher concentration (8 μM) of the withanolides resulted in necrotic cells (PI+). The effect of **9a** was more pronounced in HeLa cells than the one of withaferin A, since early apoptosis was already evidenced after 1 h of treatment. However, with **9b** a higher dose (8 μM) and a longer incubation period (2–4 h) were required to lead to apoptosis, effect that was maintained at concentrations of 12 and 16 μM. Interestingly, unlike with the other withanolides, treated cells never exhibited necrosis.

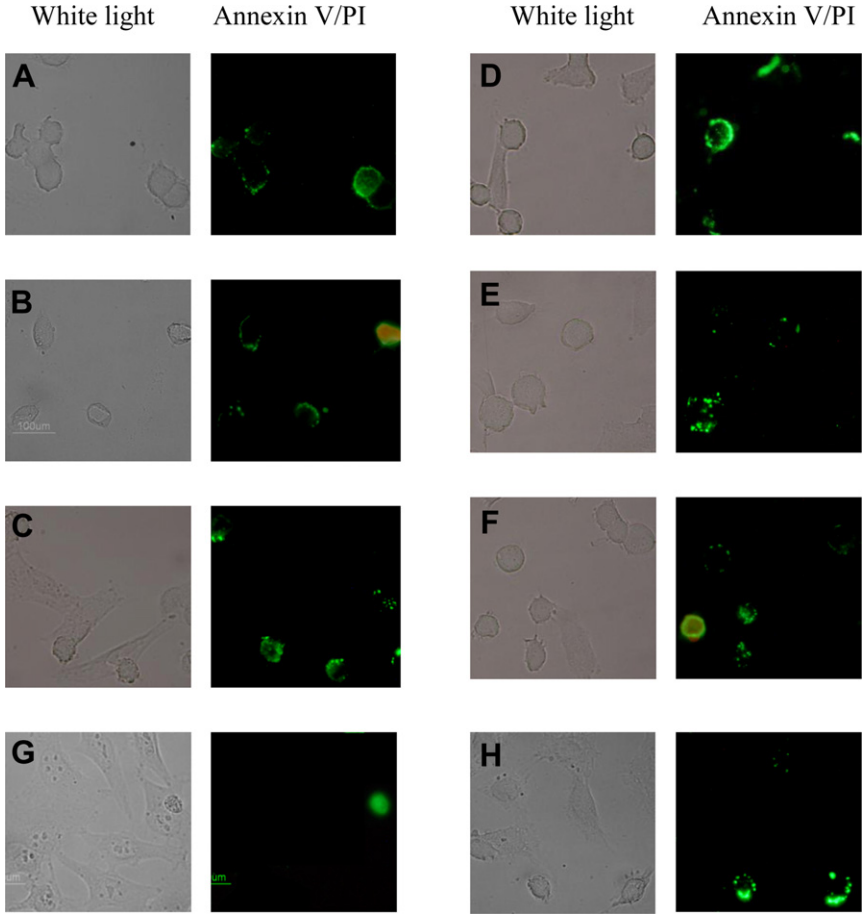

Fig. 7. Fluorescence microphotograph of withanolides treated, early apoptotic HeLa cells, characterized by phosphatidylserine (PS) extracellular membrane expression. (A) DMSO solvent control. (B) Actinomycin D at 1 μM for 1 h. (C–F) withanolides **8**, **9**, **11**, and **13** at 2 μM for 4 h (G–H) withanolides **9a** and **9b** at 8 μM for 1 and 2 h, respectively. PS flipped to the extracellular membrane was labeled with annexin V, and necrotic/late apoptotic cells were identified through PI membrane permeability.

3. Conclusion

A new series of withanolides isolated from *W. aristata*, along with three derivatives, have been evaluated as anticancer agents. Five of the assayed compounds showed a potent antiproliferative activity against three human tumor cell lines and showed higher activity than the reference anticancer agent withaferin A. Structure–activity relationships among these withanolides suggest that the silyl group gives an additional favourable effect on cytotoxicity and selectivity. Taken together, our results demonstrate that the withanolides studied in this work induce apoptosis in HeLa cells in a dose- and time-dependent manner, as evidenced by chromatin condensation, PS externalization, and most importantly caspase-3 activation, although a ladder pattern, typical for caspase activated enzymatic DNA cleavage, was not observed. These findings are consistent with data obtained by other authors for withaferin A in different cell lines. The potent capacity to induce apoptosis in cancer cells and, perhaps even more intriguingly, the induction of apoptosis by withanolide **9b** without necrosis under extreme experimental conditions, draw attention to this group of substances and call for further studies to determine their exact mechanisms of action. Our findings support the notion that these types of withanolides could be considered as active and specific anticancer agents with promising future prospects in the treatment of cancer diseases.

4. Experimental

4.1. General

Optical rotations were measured on a Perkin Elmer 241 automatic polarimeter in $CHCl_3$ at 20 °C and the $[\alpha_D]$ are given in 10^{-1} deg cm^2 g^{-1}. UV spectra were obtained on a JASCO V-560 spectrophotometer, and IR (film) spectra were measured on a Bruker IFS 55 spectrophotometer. NMR experiments were performed on a Bruker Avance 400 spectrometer and chemical shifts are shown in δ (ppm) with tetramethylsilane (TMS) as internal reference. EIMS and HREIMS were recorded on a Micromass Autospec spectrometer, and ESIMS and HRESIMS (positive mode) were measured on an LCT Premier XE Micromass Electrospray spectrometer. Purification was performed using silica gel 60 μM for column chromatography (particle size 15–40 and 63–200 μm), POLYGRAM SIL G/UV_{254} used for analytical and preparative TLC, and HPTLC-platten Nano-Sil 20 UV_{254} were purchased from Macherey–Nagel. Sephadex LH-20 for exclusion chromatography was obtained from Pharmacia Biotech. The spots were visualized by UV light and heating silica gel plates sprayed with H_2O–H_2SO_4–ACOH (1:4:20). All solvents used were analytical grade from Panreac. Reagents were purchased from Sigma Aldrich and used without further purification.

4.2. Plant material

Leaves of *W. aristata* were collected in Icod de los Vinos, Tenerife, Canary Islands (Spain), in May 2005. A voucher specimen (TFC 48.068) is deposited in the Herbarium of the Department of Botany, University of La Laguna, Tenerife, and identified by Leticia Rodríguez-Navarro.

4.3. Extraction and isolation

The air-dried powdered leaves of *W. aristata* (1.65 kg) were exhaustively extracted with CH_2Cl_2 in a Soxhlet apparatus and the solvent was evaporated at reduced pressure. The residue (71 g) was fractioned by vacuum–liquid chromatography on silica gel and eluted with hexane/EtOAc mixtures of increasing polarity (from 100:0 to 0:100) affording nine fractions, four of them (VI, VII, VIII, and IX) containing withanolides according to previous ^1H NMR analysis. Each of these fractions was subjected to column chromatography over Sephadex LH-20 (*n*-hexane/$CHCl_3$/MeOH, 2:1:1), and silica gel (CH_2Cl_2/acetone of increasing polarity). Preparative thin-layer chromatography developed with CH_2Cl_2/acetone (8.5:1.5) was used to purify the new compounds **1** (3.8 mg), **2** (4.1 mg), **3** (1.2 mg), **4** (2.3 mg), **5** (3.5 mg) **6** (3.1 mg) and **7** (1.8 mg), in addition to the known compounds 4β-hydroxy-1-oxo-5β,6β-epoxywitha-2,24-dienolide (**8**, 32.1 mg), withaferin A (**9**, 3.1 g), 2,3-dihydro-withaferin A (**10**, 2.0 mg), witharistatin (**11**, 4.8 mg), 27-deoxy-16-en-withaferin A (**12**, 3.0 mg), 4β-hydroxy-1-oxo-5β,6β-epoxy-22*R*-witha-2,14,24-trienolide (**13**, 1.5 mg), 5β,6β-epoxy-4β,17α,27-trihydroxy-1-oxowitha-2,24-dienolide (**14**, 6.0 mg), 4-dehydro-withaferin A (**15**, 1.2 mg), 2,3-dehydrosomnifericin (**16**, 2.5 mg) and 6α-chloro-5β-hydroxywithaferin A (**17**, 4.7 mg).

4.3.1. 5β,6β-Epoxy-4β,16β,27–trihydroxy-1-oxo-witha-2,17(20),24-trienolide (*1*)

White amorphous solid; $[\alpha]_D^{20}$ + 25.4 (*c* 0.6, $CHCl_3$); UV λ_{max} nm: 215; IR ν_{max} cm^{-1}: 3415, 2929, 2861, 1685, 1457, 1384, 1180, 1083, 1026, 755; ^1H NMR δ: see Table 1; ^{13}C NMR δ: see Table 2; EI/MS *m/z* %: 484 (M^+, 6), 466 (33), 448 (54), 434 (28), 391 (39), 343 (33), 281 (33), 192 (31), 151 (47), 124 (100), 95 (99), 67 (64); HREIMS: *m/z* 484.2462 (calcd for $C_{28}H_{36}O_7$ 484.2461).

4.3.2. 27-Acetoxy-5β,6β-epoxy-4β-hydroxy-1-oxo-witha-2,24-dienolide (*2*)

White lacquer; $[\alpha]_D^{20}$ + 63.4° (*c* 0.5, $CHCl_3$); UV λ_{max} nm: 215; IR ν_{max} cm^{-1}: 3748, 2928, 1701, 1540, 1458, 1397, 1256, 1066, 838; ^1H NMR δ: see Table 1; ^{13}C NMR δ: see Table 2; EI/MS *m/z*%: 512 (M^+, 7), 494 (5), 452 (9), 416 (7), 389 (21), 329 (24), 311 (25), 239 (23), 183 (25), 161 (19), 124 (100), 95 (80), 67 (43); HREIMS: *m/z* 512.2775 (calcd for $C_{30}H_{40}O_7$, 512.2774).

4.3.3. 5β,6β-Epoxy-4β-hydroxy-27-(1-formyloxy-1-methylethoxy)-1-oxo-witha-2,24-dienolide (*3*)

White lacquer; $[\alpha]_D^{20}$ + 24.3 (*c* 0.2, $CHCl_3$); UV λ_{max} nm: 220; IR ν_{max} cm^{-1}: 3438, 2931, 2870, 1700, 1460, 1396, 1320, 1186, 1019, 850, 755; ^1H NMR δ: see Table 1; ^{13}C NMR δ: see Table 2; ESIMS (positive) *m/z*%: 579 $[M + Na]^+$ (100; HRESIMS: *m/z* 579.2939 $[M + Na]^+$ (calcd. for $C_{32}H_{44}O_8Na$: 579.2934).

4.3.4. Acetoxy-5β,6β,epoxy-3,4-dihydroxy-1-oxo-witha-24-enolide (*4*)

White lacquer; $[\alpha]_D^{20}$ + 13.9 (*c* 0.39, $CHCl_3$); UV λ_{max} nm: 214; IR ν_{max} cm^{-1}: 3401, 2931, 2859, 1678, 1460, 1380, 1272, 1129, 1076, 1022, 754; ^1H NMR δ: see Table 1; ^{13}C NMR δ: see Table 2; ESIMS (positive) *m/z*%: 553 $[M + Na]^+$ (100); HRESIMS: *m/z* 553.2772 $[M + Na]^+$ (calcd. for $C_{30}H_{42}O_8Na$: 553.2777).

4.3.5. 3β,4β,5α,6β,27-Pentahydroxy-1-oxo-witha-24-enolide (*5*)

White lacquer; $[\alpha]_D^{20}$ + 28.1 (*c* 0.8, $CHCl_3$); UV λ_{max} nm: 215; IR ν_{max} cm^{-1}: 3748, 3499, 2929, 1658, 1459, 1397, 1256, 1065, 838, 756; ^1H NMR δ: see Table 1; ^{13}C NMR δ: see Table 2; ESIMS (positive) *m/z* %: 529 $[M + Na]^+$ (100); HRESIMS: *m/z* 529.2775 $[M + Na]^+$ (calcd. for $C_{28}H_{42}O_8Na$: 529.2777).

4.3.6. 4β-Formyl-6β,27-dihydroxy-1-oxo-witha-2,24-dienolide (*6*)

White lacquer; $[\alpha]_D^{20}$ + 160.8 (*c* 0.68, $CHCl_3$); UV λ_{max} nm: 220, 231; IR ν_{max} cm^{-1}: 3438, 2940, 2870, 1700, 1460, 1396, 1320, 1187, 1019, 754; ^1H NMR δ: see Table 1; ^{13}C NMR δ: see Table 2; ESIMS (positive) *m/z*%: 469 $[M - 1]^+$ (100); HRESIMS: *m/z* 469.2580 $[M - 1]^+$ (calcd. for $C_{28}H_{37}O_6$: 469.2590).

*4.3.7. 4β-Formyl-6β,27-dihydroxy-1-oxo-witha-24-enolide (**7**)*

White lacquer; $[\alpha]_D^{20}$ + 33.8 (*c* 0.21, $CHCl_3$); UV λ_{max} nm: 221; IR ν_{max} cm^{-1}: 3400, 2937, 2859, 1700, 1405, 1315, 1185, 1016, 849, 750; ^1H NMR δ: see Table 1; ^{13}C NMR δ: see Table 2; ESIMS (positive) *m/z* %: 495 $[M + Na]^+$ (100); HRESIMS: *m/z* 495.2730 $[M + Na]^+$ (calcd. for $C_{28}H_{40}O_6Na$: 495.2723).

*4.3.8. Reduction of **7***

Fifty-percent palladium hydroxide-carbon (5 mg) was added to a solution of **6** (10 mg, 0.02 mmol) in methanol (3 mL) under argon atmosphere. After hydrogenation for 1 h at room temperature under atmospheric pressure, the catalyst was removed by filtration on celite and the filtrate was concentrated in vacuo. The residue was purified using silica gel column chromatography (eluent, CH_2Cl_2/acetone, 9:1) to afford compounds **7** (1.9 mg, 20%) and **7a** (6.1 mg, 67%).

*4.3.9. 4β-Formyl-6β-hydroxy-1-oxo-witha-24-enolide (**7a**)*

White amorphous solid; $[\alpha]_D^{20}$ + 56.2 (*c* 0.10, $CHCl_3$); UV λ_{max} nm: 220; IR ν_{max} cm^{-1}: 3446, 2933, 1735, 1457, 1380, 1234, 1027, 966, 754; ^1H NMR δ: 0.77 (3H, s, Me18); 1.02 (3H, d, *J* = 6.6 Hz, Me21); 1.07 (1H, m, H9); 1.08 (1H, m, H14); 1.10 (1H, m, H12); 1.14 (1H, m, H17); 1.19 (3H, s, Me19); 1.33 (1H, m, H11); 1.39 (1H, m, H16); 1.47 (1H, m, H7α); 1.48 (1H, m, H11); 1.63 (1H, m, H15); 1.69 (1H, m, H16); 1.72 (1H, m, H15); 1.82 (1H, m, H8); 1.84 (1H, m, H3); 1.86 (1H, m, H7β); 1.91 (3H, s, Me27); 1.92 (2H, m, H23α); 1.97 (3H, s, Me28); 2.01 (1H, m, H20); 2.02 (1H, m, H12); 2.04 (1H, m, H3); 2.36 (1H, m, H2); 2.46 (1H, m, H23β); 2.60 (1H, m, H2); 4.32 (1H, t, *J* = 2.7 Hz, H6); 4.39 (1H, dt, *J* = 3.3, 13.2 Hz, H22); 9.61 (1H, s, H4); ^{13}C NMR δ: 11.9 (q, C18); 12.5 (q, C27); 13.3 (q, C19); 13.5 (q, C21); 20.6 (q, C28); 20.7 (t, C11); 22.7 (t, C3); 24.1 (t, C15); 27.3 (t, C16); 29.2 (d, C8); 29.7 (t, C23); 32.7 (t, C2); 34.4 (t, C7); 38.8 (d, C20); 39.4 (t, C12); 42.2 (d, C9); 43.2 (s, C13); 52.1 (d, C17); 52.7 (s, C10); 56.0 (d, C14); 60.7 (s, C5); 67.7 (d, C6); 78.3 (d, C22); 122.1 (s, C25); 148.9 (s, C24); 167.0 (s, C26); 204.5 (d, C4); 216.5 (s, C1); ESIMS (positive) *m/z*%: 479 $[M + Na]^+$ (100); HRESIMS: *m/z* 479.2771 $[M + Na]^+$ (calcd. for $C_{28}H_{40}O_5Na$: 479.2774).

*4.3.10. Preparation of 27-O-(tert-butyldimethylsilyl)withaferin A (**9a**)*

To a solution of diol **9** (54.0 mg, 0.12 mmol) in dry dichloromethane (5 mL) were added imidazole (9.0 mg, 0.12 mmol), 4-(*N*,*N*-dimethylamino)pyridine (14.0 mg, 0.12 mmol) and *tert*-butylchlorodimethylsilyl chloride (28.0 mg, 0.18 mmol). The reaction mixture was stirred for 2.5 h at room temperature until all starting material was consumed. The reaction was quenched with water (10 mL) and extracted with dichloromethane (3 × 10 mL). The organic layer was dried ($MgSO_4$), filtered, and evaporated. The residue was then purified by column chromatography (dichloromethane/acetone, 9:1) to give **9a** (62.1 mg, 89%): White amorphous solid; $[\alpha]_D^{20}$ + 65.2 (*c* 0.42, $CHCl_3$); UV λ_{max} nm: 215; IR ν_{max} cm^{-1}: 3446, 2933, 1735, 1457, 1380, 1234, 1027, 966, 754; ^1H NMR δ: 0.69 (3H, s, Me18); 0.89 (1H, m, H9); 0.92 (1H, m, H14); 0.98 (3H, d, *J* = 6.6 Hz, Me21); 1.06 (1H, m, H12); 1.08 (1H, m, H17); 1.16 (1H, m, H15); 1.25 (1H, m, H7α); 1.40 (3H, s, Me19); 1.41 (1H, m, H16); 1.50 (2H, m, H8, H11); 1.64 (1H, m, H15); 1.68 (1H, m, H16); 1.74 (1H, m, H11); 1.97 (2H, m, H12, H23α); 2.01 (1H, m, H20); 2.05 (3H, s, Me28); 2.16 (1H, m, H7β); 2.46 (1H, m, H23β); 2.67 (1H, br s, OH-4); 3.22 (1H, br s, H6); 3.74 (1H, d, *J* = 5.6 Hz, H4); 4.38 (1H, dt, *J* = 3.1, 13.0 Hz, H22); 4.38, 4.49 (2H, d_{AB}, *J* = 11.6 Hz, H27); 6.19 (1H, d, *J* = 10.0 Hz, H2); 6.93 (1H, dd, *J* = 5.6, 10.0 Hz, H3); TBDMSO [0.08 (6H, s); 0.88 (9H, s)]; ^{13}C NMR δ: 11.4 (q, C18); 13.1 (q, C21); 17.2 (q, C19); 20.3 (q, C28); 21.9 (t, C11); 24.0 (t, C15); 27.0 (t, C16); 29.5 (d, C8); 29.8 (t, C23); 30.9 (t, C7); 38.5 (d, C20); 39.1 (t, C12); 42.3 (s, C13); 43.9 (d, C9); 47.4 (s, C10); 51.8 (d, C17); 55.8 (d, C14); 56.9 (t, C27); 62.3 (d, C6); 63.6 (s, C5); 69.7 (d, C4); 77.9 (d, C22); 125.7 (s, C25); 132.1 (d, C2); 141.7 (d, C3); 154.3 (s, C24); 165.6 (s, C26); 202.1 (s, C1); TBDMSO [−5.5 (2 × q); 18.1 (s); 25.7 (3 × q)]; EI/MS *m/z*%: 584 (M^+, 1), 527 (100), 509 (25), 493 (5), 359 (1), 293 (2), 281 (6), 227 (23), 197 (16), 169 (7), 131 (10), 95 (12), 75 (47); HREIMS: *m/z* 584.3511 (calcd for $C_{34}H_{52}O_6Si$, 584.3533).

*4.3.11. Preparation of 27-O-(tert-butyldimethylsilyl)-4-dehydroxy-4-oxo-withaferin A (**9b**)*

A solution of **9a** (40.0 mg, 0.08 mmol) in 2.0 mL of dichloromethane was added dropwise to a chromium trioxide/pyridine complex, previously prepared by the addition of CrO_3 (62.0 mg, 0.5 mmol) to 0.1 mL of pyridine and 1.5 mL of dichloromethane at 0 °C. The reaction was stirred at room temperature for 6 h, and subsequently quenched with 2-propanol (3 drops) and filtered through a pad of celite. The filtrate was evaporated under reduced pressure, and the residue was purified by TLC chromatography (dichloromethane/acetone, 9:1) yielding **9b** (24.2 mg, 61%): White amorphous solid; $[\alpha]_D^{20}$ + 61.2 (*c* 0.49, $CHCl_3$); UV λ_{max} nm: 222; IR ν_{max} cm^{-1}: 2929, 1699, 1652, 1459, 1398, 1258, 1064, 839; ^1H NMR δ: 0.71 (3H, s, Me18); 1.00 (3H, d, *J* = 6.6 Hz, Me21); 1.02 (1H, m, H14); 1.09 (1H, m, H17); 1.17 (1H, m, H15); 1.23 (1H, m, H12); 1.35 (1H, m, H7α); 1.37 (3H, s, Me19); 1.39 (1H, m, H16); 1.45 (1H, m, H11); 1.46 (1H, m, H9); 1.62 (1H, m, H8); 1.65 (1H, m, H15); 1.69 (1H, m, H16); 1.97 (1H, m, H12); 2.00 (1H, m, H23α); 2.01 (1H, m, H11); 2.04 (1H, m, H20); 2.06 (3H, s, Me28); 2.15 (1H, m, H7β); 2.47 (1H, m, H23β); 3.42 (1H, br s, H6); 4.38 (1H, m, H22); 4.39, 4.50 (2H, d_{AB}, *J* = 11.5 Hz, H27); 6.83 (1H, d, *J* = 10.5 Hz, H2); 6.87 (1H, d, *J* = 10.5 Hz, H3); TBDMSO [0.08 (6H, s); 0.88 (9H, s)]; ^{13}C NMR δ: 11.5 (q, C18); 13.1 (q, C21); 19.0 (q, C19); 20.3 (q, C28); 23.2 (t, C11); 24.0 (t, C15); 26.9 (t, C16); 29.4 (d, C8); 29.8 (t, C23); 30.3 (t, C7); 38.5 (d, C20); 39.2 (t, C12); 42.4 (s, C13); 43.4 (d, C9); 49.6 (s, C10); 51.9 (d, C17); 55.4 (d, C14); 56.9 (t, C27); 63.3 (d, C6); 63.7 (s, C5); 77.9 (d, C22); 125.8 (s, C25); 138.9 (d, C2); 141.4 (d, C3); 154.2 (s, C24); 165.6 (s, C26); 193.8 (s, C4); 201.9 (s, C1), TBDMSO [−5.5 (2 × q); 18.1 (s); 25.7 (3 × q)]; EI/MS *m/z*%: 582 (M^+, 1), 525 (100), 509 (33), 311 (1), 297 (4), 281 (3), 253 (3), 227 (33), 197 (16), 171 (7), 151 (15), 95 (13), 75 (48); HREIMS: *m/z* 582.3383 (calcd for $C_{34}H_{50}O_6Si$, 582.3377).

*4.3.12. Preparation of 4-dehydro-withaferin A (**15**)*

A suspension of Dowex 50WX8-200 (150.0 mg) in dry acetone (4 mL) was added to a solution of compound **9b** (23 mg, 0.04 mmol) in acetone (3 mL), and the reaction mixture was stirred at room temperature for 24 h. The resin was removed by filtration through a pad of celite, and the filtrate was evaporated under reduced pressure. The residue was purified by TLC chromatography (dichloromethane/acetone, 9.5:0.5) to give **15** (22.2 mg, 99%).

4.4. Biological assays

4.4.1. Cells

HeLa (human cervix carcinoma), A-549 (human lung carcinoma), MCF-7 (human breast adenocarcinoma) and Vero (African green monkey kidney) cell lines from ATCC-LGC (American Type Culture Collection) were each grown in Dulbecco's modified Eagle's medium (DMEM) with 4.5 g/L glucose (Sigma–Aldrich), supplemented with 10% fetal bovine serum (Gibco), 1% of a penicillin–streptomycin mixture (10.000 UI/mL and 10 mg/mL, respectively), and 200 mM L-glutamine. Cells were maintained at 37 °C in 5% CO_2 and 98% humidity.

4.4.2. Cell viability assays

Viable cells were assessed using the colorimetric MTT [3-(4,5-dimethylthiazol-2-yl)-2,5-diphenyl tetrazolium bromide]

reduction assay [54]. Cell suspensions (2×10^4/200 μL/well) were seeded in DMEM, supplemented with 5% fetal bovine serum in microtiter well plates (96 wells, Iwaki, London, UK) together with the compounds, predissolved in DMSO at different concentrations, and treated for 48 or 72 h. Then, 20 μL/well of the MTT solution (5 mg/mL in phosphate buffered saline, PBS) were added and plates incubated for 3 h at 37 °C. Subsequently, the medium was aspirated and replaced with 150 μL/well of DMSO to dissolve the formazan crystals. Absorbance was measured in a microplate reader (Titertetek, Multiskan Plus II) at a wavelength of 550 nm. Solvent control cultures were considered 100% and percent of viable, treated cells were plotted against compound concentrations. The 50% cell viability value (IC_{50}) was calculated from the curve. Each experiment was performed at least three times in triplicates. Data are given in arithmetic means ± SD.

4.4.3. Detection of DNA fragmentation

HeLa cells were incubated in 24-well plates with varying concentrations of each compound or the respective volume of DMSO (solvent control) for various time periods. Cells treated with staurosporine at a concentration of 2 μM were used as positive control. After the incubation period, adherent and floating cells were collected, centrifuged at 500 g for 10 min, and washed twice with cold PBS. Then, DNA was extracted according to the manufacturer's protocol (Gen Elute™ Mammalian genomic DNA kit, Sigma–Aldrich). DNA samples were analyzed by agarose gel electrophoresis in 1.8% agarose, followed by ethidium bromide (Sigma–Aldrich) staining and visualization with UV.

4.4.4. Detection of chromatin condensation

To identify apoptotic nuclear changes (such as chromatin condensation), HeLa cells in 6-well plates were treated with the compounds at 8 μM for 12 h. After the incubation period, adherent and floating cells were collected, centrifuged at 500 g for 10 min, and washed twice with PBS, fixed in 3% paraformaldehyde (in PBS) and stained with 10 μL Hoechst 33342 (16 μg/mL) for 15 min. The slides (treated with poly-lysine) were inspected for nuclear morphological alterations and apoptotic bodies by fluorescence microscopy (*Leica*, DM 4000 B) and microphotographs taken by a coupled digital camera (Nikon DXM1200F). In order to obtain quantitative data, an area containing at least 500 cells was evaluated on each slide. Only cells containing three or more chromatin fragments were considered. Data were expressed as percent of total cell numbers.

4.4.5. Flow cytometry analysis

To estimate apoptotic events, cells with a lower DNA content than in cells in the G0/G1 phase were quantified by flow cytometry. $1–2 \times 10^6$ HeLa cells per 6-well were exposed to compounds at 24 μM for 24 h. Thereafter, adherent and floating cells were collected, centrifuged at 500 g for 10 min, washed twice with ice-cold PBS, fixed and permeabilized with ice-cold 70% ethanol, and kept at −20 °C overnight. Then, cells were centrifuged as above at 4 °C, washed twice and incubated with 100 μg/mL RNase A, together with 50 μg/mL propidium iodide (PI), in the dark at room temperature for 1 h. At least 1×10^4 cells from each sample were analyzed in an Epics XL-MCL flow cytometer (Beckman Coulter, CA).

4.4.6. Caspase-3 activity assay

Caspase-3 activity was carried out using a colorimetric assay kit (Molecular Probes/Invitrogen, Carlsbad, CA) according to manufacturer's protocol. HeLa cells (1×10^6/6- well) were incubated for the indicated time periods in the presence or absence of different concentrations of the compounds or of 2 μM of staurosporine, used as positive control. Adhered and floating cells were then harvested, centrifuged at 300 g for 5 min, and washed twice in cold PBS. The pellets were lysed at 4 °C in 100 μL of lysis buffer for 10 min. Lysates were centrifuged at 16,000 g for 2 min, and total protein in supernatants was determined by Bradford assay (Bio-Rad, Hercules, CA). Caspase-3 activity assays were performed in 96 well plates by incubating 50 μg of protein in 50 μL of reaction buffer and 5 μL of the 4 mM chromogenic substrate, Ac-DEVD-*p*NA, at 37 °C for 2 h. Absorbance of released *p*-nitroaniline was measured at 405 nm (Tecan Group Ltd., Männedorf, Switzerland) and activity of caspase-3 evaluated by calculating OD (optical density) ratios of treated/untreated samples. Experiments were performed in triplicates.

4.4.7. Phosphatidylserine labeling

1.6×10^6 HeLa cells each were grown on coverslips in 24-wells and treated with varying concentrations of the compounds or the respective volume of DMSO (solvent control) or actinomycin D at 1 μM (positive control) for different time periods. Phosphatidylserine externalization and cell permeability were assessed by Annexin V/PI double staining (Vybrant® Apoptosis Assay Kit ≠2, Invitrogen, Molecular Probes™), according to the manufacturer's instructions. Apoptotic cells were recognized by fluorescence microscopy (*Leica*, DM 4000 B) and microphotographs taken by a coupled digital camera (Nikon DXM1200F). Annexin V^+PI^- cells were considered as early apoptotic while Annexin V^+PI^+ cells as late apoptotic/necrotic.

4.4.8. Statistical analysis

All results were expressed as means ± SD. Significance differences between groups were determined using unpaired Student's *t*-test. Significance was set at $p < 0.05$.

Acknowledgments

This study was supported by the Agencia Canaria de Investigación, Innovación y Sociedad de la Información (C200801000049). G.G.LL. thanks the Gobierno Autónomo de Canarias for the fellowship. Thanks are also due to Leticia Rodríguez-Navarro, Department of Botany, University of La Laguna for the identification of the plant.

Appendix A. Supplementary material

Supplementary material associated with this article can be found, in the online version, at doi:10.1016/j.ejmech.2012.05.032.

References

[1] B.M. Bhuwan, K.T. Vinod, Eur. J. Med. Chem. 46 (2011) 4769–4807.
[2] D.J. Newman, G.M. Cragg (Functional Molecules from Natural Sources), Spec. Publ. Roy. Soc. Chem. 320 (2011) 3–36.
[3] E. Glotter, Nat. Prod. Rep. 8 (1991) 415–440.
[4] L.-X. Chen, H. He, F. Qiu, Nat. Prod. Rep. 28 (2011) 705–740.
[5] W. Hu, J.J. Kavanagh, Lancet Oncol. 4 (2003) 721–729.
[6] S. Srinivasan, R.S. Ranga, R. Burikhanov, S. Han, D. Chendil, Cancer Res. 67 (2007) 246–253.
[7] S. Koduru, R. Kumar, S. Srinivasan, M.B. Evers, C. Damodaran, Mol. Cancer Ther. 9 (2010) 202–210.
[8] S.D. Stan, E. Hahm, R. Warin, S.V. Singh, Cancer Res. 68 (2008) 7661–7669.
[9] C. Mandal, A. Dutta, A. Mallick, S. Chandra, L. Misra, R.S. Sangwan, C. Mandal, Apoptosis 13 (2008) 1450–1464.
[10] Y. Yu, A. Hamza, T. Zhang, M. Gu, P. Zou, B. Newman, Y. Li, A.A.L. Gunatilaka, C. Zhan, D. Sun, Biochem. Pharmacol. 79 (2010) 542–551.
[11] T.J. Lee, H.J. Um, D.S. Min, J.W. Park, K.S. Choid, T.K. Kwon, Free Radic. Biol. Med. 46 (2009) 1639–1649.
[12] A.K. Samadi, X. Tong, R. Mukerji, H. Zhang, B.N. Timmermann, M.S. Cohen, J. Nat. Prod. 73 (2010) 1476–1481.
[13] N. Malara, D. Focá, F. Casadonte, M.F. Sesto, L. Macrina, L. Santoro, M. Scaramuzzino, R. Terracciano, R. Savino, Cell Cycle 7 (2008) 3235–3245.
[14] J.H. Oh, T.J. Lee, S.H. Kim, Y.H. Choi, S.H. Lee, J.M. Lee, Y.H. Kim, J.W. Park, T.K. Kwon, Apoptosis 13 (2008) 1494–1504.

[15] E.-R. Hahm, M.B. Moura, E.E. Kelley, B.V. Houten, S. Shiva, S.V. Singh, PloS ONE 6 (2011) e23354.
[16] E. Mayola, C. Gallerne, D.D. Esposti, C. Martel, S. Pervaiz, L. Larue, B. Debuire, A. Lemine, C. Brenner, Ch. Lemaire, Apoptosis 16 (2011) 1014–1027.
[17] S.J. Cruz, Más de 100 Plantas Medicinales. Medicina Popular Canaria Monografías. Las Palmas de Gran Canaria, Imprenta Pérez Galdós, Las Palmas de Gran Canaria (2007).
[18] A.G. González, J.L. Bretón, J. Trujillo, An. Quím. 68 (1972) 107–108.
[19] A.G. González, J.L. Bretón, J.M. Trujillo, An. Quím. 70 (1974) 64–68.
[20] A.G. González, J.L. Bretón, J. Trujillo, An. Quím. 70 (1974) 69–73.
[21] A.G. González, V. Darias, D.A. Martín-Herrera, M.C. Suárez, Fitoterapia 53 (1982) 85–88.
[22] D. Benjumea, D. Martín-Herrera, S. Abdala, J. Guitiérrez-Luis, W. Quiñones, D. Cardona, F. Torres, F. Echeverri, J. Ethnopharmacol. 123 (2009) 351–355.
[23] G.G. LLanos, L.M. Araujo, I.A. Jiménez, L.M. Moujir, J.T. Vázquez, I.L. Bazzocchi, Steroids 75 (2010) 974–981.
[24] I. Kirson, E. Glotter, D. Lavie, J. Chem. Soc. (C) (1971) 2032–2044.
[25] S. Habtemariam, A.I. Gray, Planta Med. 64 (1998) 275–276.
[26] PC Model from Serena Sotware, P.O. Box 3076, Bloomington, IN 47402-3076, version 9.0 with MMX force field.
[27] L. Misra, P. Mishra, A. Pandey, R.S. Sangwan, N.S. Sangwan, R. Tuli, Phytochemistry 69 (2008) 1000–1004.
[28] D. Alfonso, I. Kapetanidis, J. Nat. Prod. 54 (1991) 1576–1582.
[29] S.W. Pelletier, N.V. Mody, J. Nowacki, J. Bahattacharyya, J. Nat. Prod. 42 (1979) 512.
[30] S.W. Pelletier, G. Gebeyehu, J. Nowacki, M.V. Naresh, Heterocycles 15 (1981) 317–320.
[31] B. Jayaprakasam, M.G. Nair, Tetrahedron 59 (2003) 841–849.
[32] S. Ahmad, A. Malik, R. Yasmin, N. Ullah, W. Gul, P.M. Khan, H.R. Nawaz, N. Afza, Phytochemistry 50 (1999) 647–651.
[33] S.S. Nittala, D. Lavie, J. Chem. Soc. Perkin Trans. (1982) 2835–2839.
[34] I. Kirson, E. Glotter, A. Abraham, D. Lavie, Tetrahedron 26 (1970) 2209–2219.
[35] L. Misra, P. Lal, R.S. Sangwan, N.S. Sangwan, G.C. Uniyal, R. Tuli, Phytochemistry 66 (2005) 2702–2707.
[36] M.I. Choudhary, S. Yousuf, S.A. Nawaz, S. Ahmed, A. Rahman, Chem. Pharm. Bull. 52 (2004) 1358–1361.
[37] M.I. Choudhary, S. Abbas, S.A. Jamal, Atta-ur-Rahman, Heterocycles 42 (1996) 555–563.
[38] L. Misra, P. Lal, N.D. Chaurasia, R.S. Sangwan, S. Sinha, R. Tuli, Steroids 73 (2008) 245–251.
[39] B. Jayaprakasam, Y. Zhang, N.P. Seeram, M.G. Nair, Life Sci. 74 (2003) 125–132.
[40] J. Fuska, A. Fuskova, J.P. Rosazza, A.W. Nicholas, Neoplasma 31 (1984) 31–36.
[41] Y.-M. Xu, M.T. Marron, E. Seddon, S.P. McLaughlin, D.T. Ray, L. Whitesell, A.A.L. Gunatilaka, Bioorg. Med. Chem. 17 (2009) 2210–2214.
[42] A.G. Damu, P.-Ch. Kuo, Ch.-R. Su, T.-H. Kuo, T.-H. Chen, K.F. Bastw, K.-H. Lee, T.-S. Wu, J. Nat. Prod. 70 (2007) 1146–1152.
[43] P.-W. Hsieh, Z.-Y. Huang, J.-H. Chen, F.-R. Chang, Ch.-Ch. Wu, Y.-L. Yang, M.Y. Chiang, M.-H. Yen, S.-L. Chen, H.-F. Yen, T. Lübken, W.-Ch. Hung, Y.-Ch. Wu, J. Nat. Prod. 70 (2007) 747–753.
[44] T. Meyer, L. Nindl, T. Schmook, C. Ulrich, W. Sterry, W.E. Stockfleth, Br. J. Dermatol. 149 (2003) 9–14.
[45] C.B. Bortner, N.B.E. Oldenburg, J.A. Cidlowski, Trends Cell Biol. 5 (1995) 21–26.
[46] X. Wang, F.F. Becker, P.R. Gascoyne, Biochim. Biophys. Acta 1564 (2002) 412–420.
[47] G. Lizard, V. Deckert, L. Dubrez, M. Moisant, P. Gambert, L. Lagrost, Am. J. Pathol. 148 (1996) 1625–1638.
[48] S. Van Cruchten, W. Van den Broeck, Anat. Histol. Embryol. 31 (2002) 214–223.
[49] A.G. Porter, R.U. Jänicke, Cell Death Differ. 6 (1999) 99–104.
[50] U.J. Reiner, M.L. Sprengart, M.R. Wati, A.G. Poter, J. Biol. Chem. 273 (1998) 9357–9360.
[51] V. Senthil, S. Ramavedi, V. Venkatakrishnan, P. Giridharan, B.S. Lakshmi, R.A. Vishwakarma, A. Balakrishnan, Chem. Biol. Interact. 167 (2007) 19–30.
[52] S. Sowmyalakshmi, S.R. Rama, B. Ravshan, S.H. Seong, C. Damodaran, Cancer Res. 67 (2007) 246–253.
[53] M.K. Callahan, P. Williamson, R.A. Schlegel, Cell Death Differ. 7 (2000) 645–653.
[54] T. Mosmann, J. Immunol. Methods 65 (1983) 55–63.